ISSN 1029-9599, Physical Mesomechanics, 2016, Vol. 19, No. 4, pp. 355–364. © Pleiades Publishing, Ltd., 2016.
Original Text © M.R.M. Aliha, F. Berto, A. Bahmani, Sh. Akhondi, A. Barnoush, 2016, published in Fizicheskaya Mezomekhanika, 2016, Vol. 19, No. 4, pp. 92–100.

Fracture Assessment of Polymethyl Methacrylate Using Sharp Notched Disc Bend Specimens under Mixed Mode I + III Loading

M. R. M. Aliha[1]*, F. Berto[2,3], A. Bahmani[1], Sh. Akhondi[1], and A. Barnoush[3]

[1] *Welding and Joining Research Center, School of Industrial Engineering, Iran University of Science and Technology, Narmak, Tehran, 16846-13114 Iran*
[2] *Department of Management and Engineering, University of Padova, Vicenza, 36100 Italy*
[3] *Department of Engineering Design and Materials, Norwegian University of Science and Technology, Trondheim, 7491 Norway*
** e-mail: m_aliha@yahoo.com, mrm_aliha@iust.ac.ir*

Received February 29, 2016

Abstract—Mixed mode I/III behavior of Perspex (polymethyl methacrylate (PMMA)) is studied experimentally and theoretically in this research using a new and simple laboratory test configuration. The specimen is a circular disc containing a sharp V-notch along the diameter that is loaded by the conventional three-point bend fixture. The critical values of notch stress intensity factors ($K_{\mathrm{I}}^{\mathrm{V}}$ and $K_{\mathrm{III}}^{\mathrm{V}}$) were obtained for the whole combinations of modes I and III simply by changing the notch inclination angle relative to the loading rollers. The value of notch fracture toughness under pure or dominantly tension loads was greater than its corresponding value under mode III or dominantly torsion loads. The experimental results were also predicted very well by employing the local strain energy density (SED) criterion.

DOI: 10.1134/S1029959916040020

Keywords: PMMA, mixed mode I/III loading, notch fracture toughness, SED criterion

1. INTRODUCTION

Integrity assessment of engineering components and structures in the presence of high stress concentration sources such as notches or sharp cracks, is an interesting subject and of practical importance. Different aspects associated with fracture of cracked or notched components have been extensively investigated in the past by means of laboratory test specimens under controlled testing conditions and by means of model materials. Polymethyl methacrylate (PMMA) is a well-known model material for investigating brittle fracture phenomenon. Optical transparency of PMMA makes ease study of fracture initiation and its propagation trajectory under any desired complex loading situation. Fracture test specimen in any arbitrary shapes can be easily manufactured from a PMMA sheet by laser cutting or water jet machines. Fracturing load of such material with laboratory scale samples is relatively low and hence fracture toughness experiments on PMMA can be conducted even by means of conventional and low capacity testing machines. Consequently, a large number of researchers have used this material in their experimental fracture studies. Based on the principles of fracture mechanics a cracked or notched body can experience mode I (opening or tensile load), mode II (in-plane sliding or shear deformation), mode III (out-of-plane sliding or tearing deformation) or any combinations of these three basic modes. Under each loading condition, study of the onset of fracture initiation, the direction of fracture growth and the path of brittle fracture are interesting subjects and hence PMMA has been widely used in the past for investigating the mentioned problems. Using different test specimens such as (center cracked tensile plate [1], single edge notched bend beam [2, 3], diametral compressed Brazilian disc [4], semicircular bend [5–7], triangular specimen subjected to three-point bending [8], diagonally loaded square plate [9], compact tension-shear specimen [10]

and etc.), mode I, mode II and mixed mode I/II fracture behavior of PMMA has been studied experimentally and extensive data are available in the literature for K_{Ic} and K_{IIc} of cracked PMMA samples. Furthermore, there are also several research papers dealing with the fracture behavior of notched PMMA specimens under different loading modes. For example, mode I and mixed mode I/II notch fracture toughness of PMMA has been determined using some test configurations such as edge notched three point bend beam and compact tension specimens and by considering different U- and V-notch geometries [11–14]. However, in comparison with the mixed mode I/II loading case, there are relatively fewer experimental results presented for mode III or mixed mode I/III fracture behavior of PMMA [15, 16]. In other words, only a limited number of test specimens are available for mixed mode I/III studies. However, the available test specimens have two major limitations: (i) many of them are not able to introduce full combinations of modes I and III [17, 18], (ii) some of them have complex geometries and require difficult preparation process and complex testing rigs or fixtures [19, 20]. In order to overcome these two drawbacks, in this paper a simple and suitable disc type bend test configuration is proposed for mixed mode I/III fracture toughness studies. The applicability of the suggested notched specimen is then examined by performing some fracture tests on PMMA. It is shown that the suggested specimen can easily introduce complete range of modes, including mixed ones, from pure mode I to pure mode III. Furthermore, it is demonstrated that the notch fracture toughness test data obtained from the tested PMMA can be predicted by means of the strain energy density (SED) criterion [21, 22].

2. SUGGESTED MIXED MODE I/III FRACTURE SPECIMEN

As shown in Fig. 1, the proposed specimen is a circular disc of diameter D and height B which contains a sharp edge notch of angle 2α and depth a along one side of disc. The specimen is subjected to three-point bend loading with loading span of $2S$, in which the bottom loading supports are symmetric with respect to the top roller. Hence, the specimen is so called edge notched disc bend (ENDB). The state of notch flank deformation in the ENDB specimen can be controlled by the angle β, defined in Fig. 1. When β is zero (i.e. symmetric ENDB shown in Figs. 1a and 1c), the specimen would be subjected to pure mode I due to symmetry of both geometry and loading relative to the notch plane. By increasing β, the specimen experiences mixed mode opening and out-of-plane sliding deformation.

Recently Aliha and coworkers [23, 24], studied numerically this specimen containing a sharp crack and computed its stress intensity factors for different $a/B, D/2S$ and β values. They showed that the mode II component has negligible value relative to K_I and K_{III} in this specimen and the full combinations of mode I/III mixities can be achieved by changing the crack inclination angle. However, in practice the artificial notches created by means of razor or thin saw blades in laboratory fracture study of brittle materials

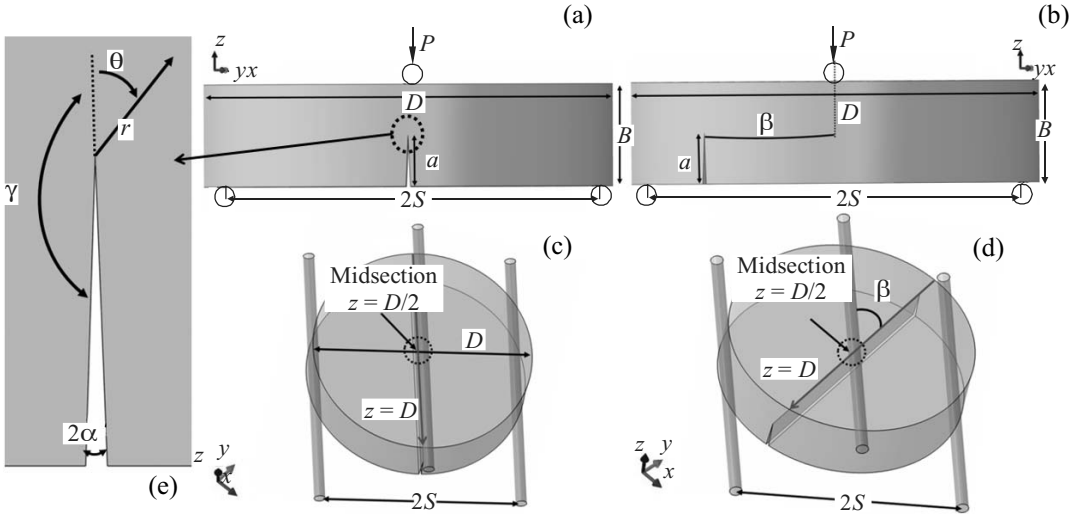

Fig. 1. Geometry and loading condition of the ENDB specimen containing a sharp notch of angle 2α for introducing pure mode I, pure mode III and mixed mode I/III conditions.

like PMMA are not real sharp cracks and hence in order to provide more realistic estimations for fracture behavior of such test specimens and investigating the possible effects of notch type, it is better to consider the created sluts as sharp notch instead of real crack. Hence in the following, by assuming a sharp notch in the ENDB specimen, the notch stress intensity factors (NSIFs) are computed for this specimen using finite element analyses and for different mixed mode I/III loading conditions.

3. NSIF CALCULATION FOR THE ENDB SPECIMEN

Based on the William's expression, the stress field for a sharp notch in a polar coordinate (as defined in Fig. 1) can be written as following equations extracted from [25–28]:

$$\sigma_{rr} = \frac{K_{\mathrm{I}}^{\mathrm{V}}}{r^{1-\lambda_{\mathrm{I}}}} f_{rr}(\theta) + \frac{K_{\mathrm{II}}^{\mathrm{V}}}{r^{1-\lambda_{\mathrm{II}}}} g_{rr}(\theta), \quad (1)$$

$$\sigma_{\theta\theta} = \frac{K_{\mathrm{I}}^{\mathrm{V}}}{r^{1-\lambda_{\mathrm{I}}}} f_{\theta\theta}(\theta) + \frac{K_{\mathrm{II}}^{\mathrm{V}}}{r^{1-\lambda_{\mathrm{II}}}} g_{\theta\theta}(\theta), \quad (2)$$

$$\sigma_{r\theta} = \frac{K_{\mathrm{I}}^{\mathrm{V}}}{r^{1-\lambda_{\mathrm{I}}}} f_{r\theta}(\theta) + \frac{K_{\mathrm{II}}^{\mathrm{V}}}{r^{1-\lambda_{\mathrm{II}}}} g_{r\theta}(\theta), \quad (3)$$

$$\sigma_{zr} = \frac{K_{\mathrm{III}}^{\mathrm{V}}}{r^{1-\lambda_{\mathrm{III}}}} \sin(\lambda_{\mathrm{III}}\theta), \quad (4)$$

$$\sigma_{z\theta} = \frac{K_{\mathrm{III}}^{\mathrm{V}}}{r^{1-\lambda_{\mathrm{III}}}} \cos(\lambda_{\mathrm{III}}\theta), \quad (5)$$

in which $\lambda_{\mathrm{I}}, \lambda_{\mathrm{II}}$ and λ_{III} are the eigenvalues that depend on the notch angle 2α and f, g are angular functions given in [29]. The parameters K_i^{V} (i = I, II and III) are the modes I, II and III notch stress intensity factors and can be determined from the following equations:

$$K_{\mathrm{I}}^{\mathrm{V}} = \lim_{r\to 0}[(2\pi r^{1-\lambda_{\mathrm{I}}})\sigma_{\theta\theta}], \quad (6)$$

$$K_{\mathrm{II}}^{\mathrm{V}} = \lim_{r\to 0}[(2\pi r^{1-\lambda_{\mathrm{II}}})\sigma_{r\theta}], \quad (7)$$

$$K_{\mathrm{III}}^{\mathrm{V}} = \lim_{r\to 0}[(2\pi r^{1-\lambda_{\mathrm{III}}})\sigma_{zr}]. \quad (8)$$

The values of $\lambda_{\mathrm{I}}, \lambda_{\mathrm{II}}$ and λ_{III} can also be determined by solving the below equations [30]:

$$\sin(2\lambda\gamma) + \lambda\sin(2\gamma) = 0 \text{ (mode I)}, \quad (9)$$

$$\sin(2\lambda\gamma) - \lambda\sin(2\gamma) = 0 \text{ (mode II)}, \quad (10)$$

$$\cos(\lambda\gamma) = 0 \text{ (mode III)}. \quad (11)$$

Corresponding values of $\lambda_{\mathrm{I}}, \lambda_{\mathrm{II}}$ and λ_{III} for small notch opening angles (up to $2\alpha = 15°$) were determined as 0.5 from Eqs. (9) to (11), implying that singularity character of sharp notches is the same as cracks. Thus as a good engineering assumption such notches can be considered as a real crack.

Meanwhile, $\sigma_{\theta\theta}, \sigma_{r\theta}$ and τ_{zr} in Eqs. (6) to (8) are the polar stress components on the notch bisector line (i.e. along $\theta = 0°$). Therefore, in order to compute the NSIFs for the investigated ENDB specimen, it is necessary to obtain these three stress components along the nodes located at $\theta = 0°$ line. By performing a static finite element analysis for each loading angle β, the required stress components were obtained numerically. Following geometrical parameters were considered for the finite element modeling of the sharp notched ENDB specimen: D = 70 mm, B = 20 mm, a = 8 mm, $2S$ = 66.5 mm and $2\alpha = 5°$. The material properties of PMMA was also used in finite element models as ν = 0.3 and E = 2950 MPa. Figure 2 shows the finite element model of the ENDB specimen and a zoomed view of the sharp notch tip. The model was created by means of 65 000 solid C3D20 elements in the ABAQUS code, in which very fine elements were employed along the notch front.

The variations $\sigma_{\theta\theta}, \sigma_{r\theta}$ and σ_{zr} stress components along the notch bisector have been presented in Fig. 3 for typical β angle of 53° and for different crack front locations defined by z in Fig. 1. The curves in these graphs have been normalized to the corresponding value of stress component obtained at the midsection (i.e. $z = D/2$) and at $r = 0$. It is seen from this figure that the notch tip stress field depends noticeably on the front location and in general a complex 3D stress state is seen at the tip of notch. But as one moves along the ligament, most of the stress components tends towards zero. Figure 4 shows the results of modes I, II and III NSIFs along the crack front computed from Eqs. (6) to (8) for different crack inclination angles. The presented results have been normalized by divid-

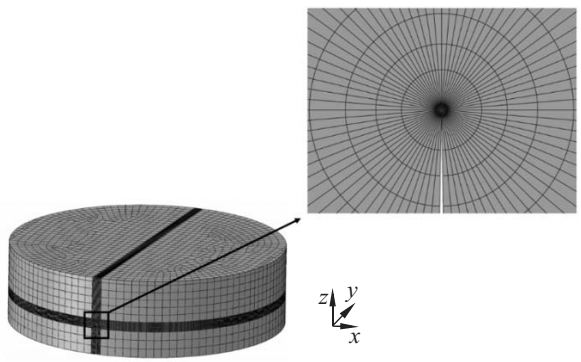

Fig. 2. Finite element model of the ENDB specimen and a zoomed view of notch tip.

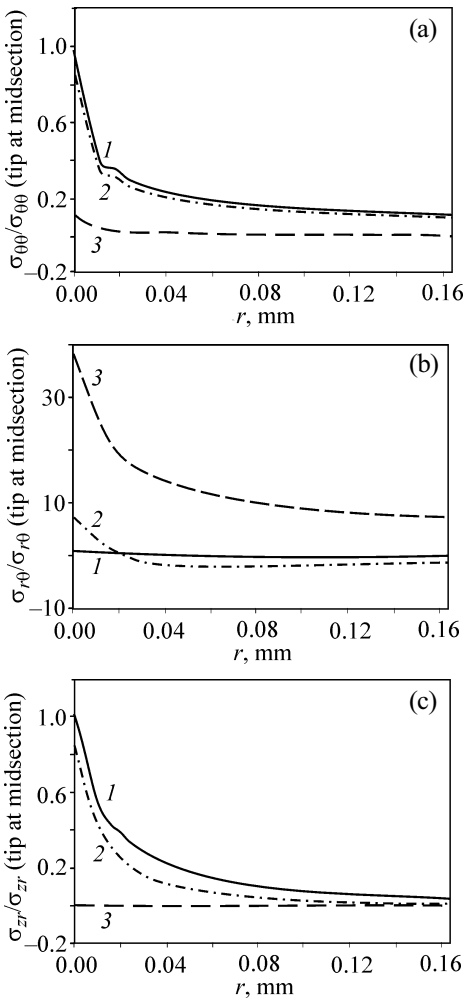

Fig. 3. Variations of stress components along the notch line and for different through thickness locations ($z = D/2$ (*1*), $3D/4$ (*2*), D (*3*)).

ing the NSIFs to the $K_{\mathrm{I}}^{\mathrm{V}}$ at 0° (i.e. the value of K_{I} component at the midsection and $\beta = 0°$). According to this figure, in general, three-dimensional effects are observed for the distribution of NSIFs along the notch front. By ignoring the unreliable results for the corner edges of the specimen due to edge effects (i.e. typically for $z < 7$ mm and $z > 63$ mm), it is seen that the mode I and mode III NSIFs increase gradually by moving towards the midsection but mode II component (i.e. $K_{\mathrm{II}}^{\mathrm{V}}$) tends to zero. Thus, at the midsection of specimen (i.e. $z = 35$ mm), both $K_{\mathrm{I}}^{\mathrm{V}}$ and $K_{\mathrm{III}}^{\mathrm{V}}$ components become maximum but $K_{\mathrm{II}}^{\mathrm{V}}$ is zero for any crack inclination angle β. In other words, although both modes II and III shear components are always coupled in a cracked or notched specimen [31–33], but the value of mode II component becomes negligible in the midsection zone of the ENDB specimen. Therefore, the ENDB specimen at the onset of fracture would experience mixed mode I/III loading in this critical point (which corresponds to the point of fracture initiation). When β is zero, it is seen from Fig. 4a that both $K_{\mathrm{II}}^{\mathrm{V}}$ and $K_{\mathrm{III}}^{\mathrm{V}}$ components are zero but $K_{\mathrm{I}}^{\mathrm{V}}$ is nonzero that indicates the ENDB specimen is subjected to pure mode I loading. Conversely, at a specific angle β (for instance $\beta = 65°$ in the case of ENDB of this research) which depends on the specimen geometry and notch length, $K_{\mathrm{I}}^{\mathrm{V}}$ becomes zero at the midsection but $K_{\mathrm{III}}^{\mathrm{V}}$ is nonzero (Fig. 4d). This situation corresponds to pure mode III loading. Any inclination angle between zero and β_{III} (i.e. pure mode III inclination angle) may introduce an intermediate mode I/III mixity. As a con-

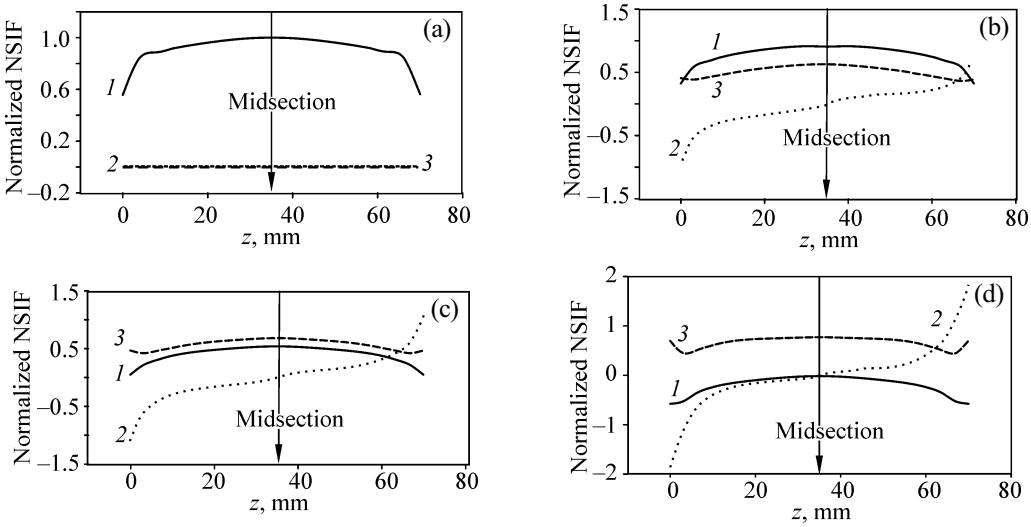

Fig. 4. Variations of normalized notch stress intensity factors ($K_{\mathrm{I}}^{\mathrm{V}}$, $K_{\mathrm{II}}^{\mathrm{V}}$ and $K_{\mathrm{III}}^{\mathrm{V}}$) for the investigated notched ENDB specimen thorough the crack front. $K_{\mathrm{I}}/K_{\mathrm{Im}}$ (*1*), $K_{\mathrm{II}}/K_{\mathrm{Im}}$ (*2*) and $K_{\mathrm{III}}/K_{\mathrm{Im}}$ (*3*) at 0°.

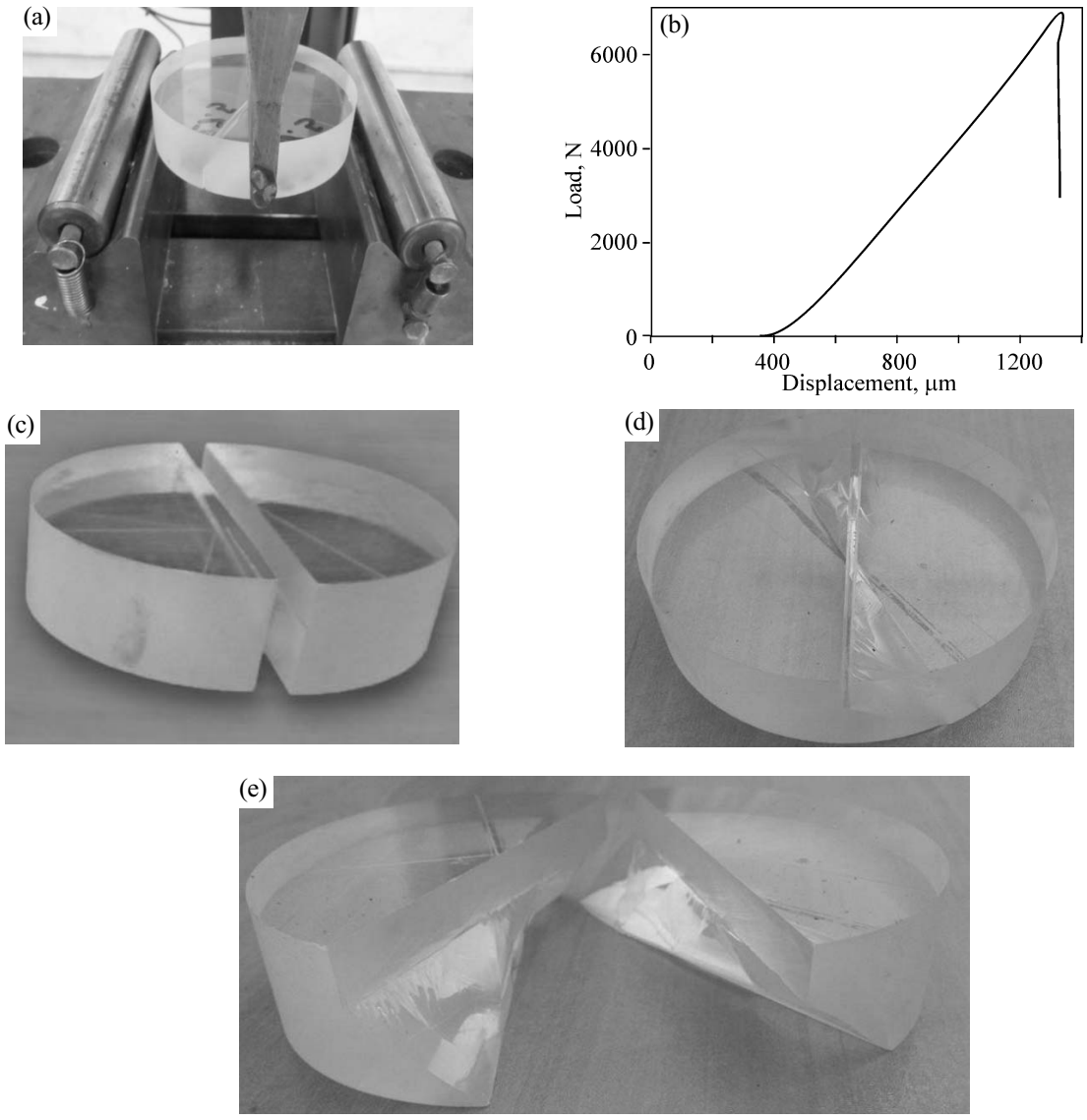

Fig. 5. Test setup (a), typical load-displacement (b) and fracture trajectories of the ENDB specimen made of PMMA (c–e): pure mode I (c), mixed mode I/III (d), fracture surface (e).

clusion, the ENDB specimen can be used for producing the whole mode mixities from pure mode I to pure mode III notch fracture modes simply by setting the notch inclination angle β in appropriate value relative to the vertical direction. In the next sections, the practical applicability of the suggested notched ENDB specimen is investigated via some fracture experiments on PMMA and also theoretical studies.

4. NOTCH FRACTURE TOUGHNESS EXPERIMENTS ON PMMA

In order to conduct the experiments, several disc specimens with radius of 35 mm and thickness of 20 mm were cut from a PMMA sheet using laser cutting machine. Then an edge notch of 8 mm depth were cut in one side of each disc by means of a very narrow rotary saw blade. The loading span (i.e. 2*S*) was considered equal to 64.75 mm. The manufactured ENDB specimens were then placed inside a three-point bend fixture as shown typically in Fig. 5a with different inclination angles β (in the range of zero and 65°) and were loaded monotonically until the fracture of specimens. All the tested ENDB samples had linear and elastic behavior and showed different trajectories depending on the mode I and III mixity. Figures 5b and 5c show typical load-displacement curves and fracture trajectories observed for the tested ENDB specimens made

of PMMA under mixed mode I and III. It is seen from Fig. 5c that the pure mode I fracture path is along the plane of initial notch, but by increasing the contribution of mode III component, fracture extends along out of the plane of initial notch and its deviation from the initial notch plane becomes more by moving toward pure mode III.

The notch fracture toughness experiments were conducted for six β angle of 0°, 27°, 44°, 53°, 60° and 65° and for each angle three replicates of ENDB specimen made of PMMA were tested. By applying the critical fracture load (i.e. the peak load) of each specimen to the finite element models of the ENDB specimen, the corresponding values of polar stresses in front of the notch was obtained from the finite element analyses. Then, the critical values of NSIFs at the onset of fracture were obtained from Eqs. (6) to (8). Table 1 presents the corresponding values of critical notch stress intensity factors for different notch inclination angles in the investigated ENDB specimens. This table obviously reveals that the ENDB specimen is able to introduce full combinations of mode I/III mixities from pure mode I to pure mode III in PMMA when β changes from zero to 65°. Mode II component was also nearly zero in all mode mixities. By increasing β, the value of $K_{\mathrm{I}}^{\mathrm{V}}$ decreases and conversely $K_{\mathrm{III}}^{\mathrm{V}}$ increases. However, the value of critical NSIF in this specimen under pure mode I is noticeably greater than its corresponding value under pure mode III loading case. In the next section the experimental results are predicted theoretically using an energy-based fracture criterion.

Table 1. Average of mixed mode I/III notch fracture toughness results for the PMMA tested with ENDB specimen

β	Average of P_{c}, N	$K_{\mathrm{I}}^{\mathrm{V}}$, MPa×m$^{1/2}$	$K_{\mathrm{II}}^{\mathrm{V}}$, MPa×m$^{1/2}$	$K_{\mathrm{III}}^{\mathrm{V}}$, MPa×m$^{1/2}$
0°	2784.50	1.92	0	0.00
27°	3512.75	2.00	0	0.55
44°	6267.00	1.73	0	1.37
53°	6856.00	1.03	0	1.31
60°	8636.75	0.50	0	1.50
65°	9181.25	0.00	0	1.40

5. STRAIN ENERGY DENSITY AVERAGED OVER A CONTROL VOLUME. THE FRACTURE CRITERION

With the aim to assess the fracture load in notched PMMA components, an appropriate fracture criterion is required which has to be based on the mechanical behavior of material around the notch tip. In this section, a criterion proposed by Lazzarin and co-authors [21, 22] based on the strain energy density is briefly described.

The averaged strain energy density criterion as presented in Refs. [22, 34] states that brittle failure occurs when the mean value of the strain energy density over a given control volume is equal to a critical value W_{c}. This critical value varies from material to material but it does not depend on the notch geometry and sharpness. The control volume is considered to be dependent on the ultimate tensile strength σ_{t} and the fracture toughness K_{Ic} in the case of brittle or quasi-brittle materials subjected to static loads.

The method based on the averaged SED was formalized and applied first to sharp (zero radius) V-notches under mode I and mixed mode I/II loading [21] and later extended to blunt U- and V-notches [22, 35, 36]. When dealing with cracks, the control volume is a circle of radius R_{c} centered at the crack tip (Fig. 6a). Under plane strain conditions, the radius R_{c} can be evaluated according to the following expression:

$$R_{\mathrm{Ic}} = \frac{(1+\nu)(5-8\nu)}{4\pi}\left(\frac{K_{\mathrm{Ic}}}{\sigma_{\mathrm{t}}}\right)^2, \qquad (12)$$

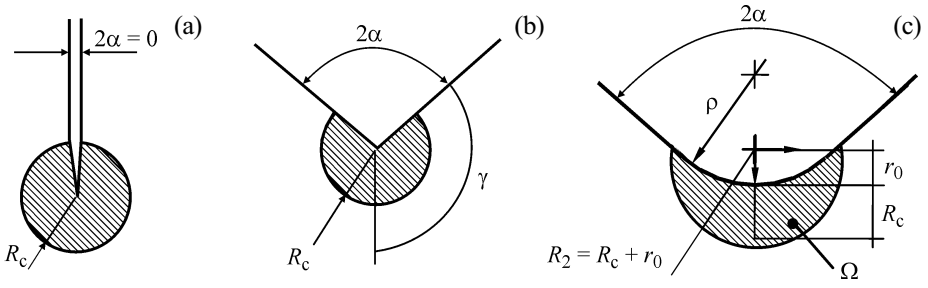

Fig. 6. Control volume for crack (a), sharp V-notch (b) and blunt V-notch (c) under mixed mode I/III loading. Distance $r_0 = \rho \times (\pi - 2\alpha)/(2\pi - 2\alpha)$.

where K_{Ic} is the fracture toughness, ν is the Poisson ratio, and σ_t is the ultimate tensile stress of a plane specimen.

For a sharp V-notch, the critical volume becomes a circular sector of radius R_c centred at the notch tip (Fig. 6b). When only failure data from open V-notches are available, R_c can be determined on the basis of some relationships reported in [22], where K_{Ic} is substituted by the critical value of the notch stress intensity factors as determined at failure from sharp V-notches.

Dealing here with sharp notches under torsion loading, the control radius R_{3c} can be estimated by means of the following equation [31]:

$$R_{3c} = \left(\sqrt{\frac{e_3}{1+\nu}} \frac{K_{IIIc}}{\tau_t} \right)^{1/(1-\lambda_3)}, \qquad (13)$$

where K_{IIIc} is the mode III critical notch stress intensity factor and τ_t is the ultimate torsion strength of the unnotched material. Moreover, e_3 is the parameter that quantifies the influence of all stresses and strains over the control volume, and $(1-\lambda_3)$ is the degree of singularity of the linear elastic stress fields [29], which depends on the notch opening angle. Values of e_3 and λ_3 are 0.4138 and 0.5 for the crack or very sharp notch cases ($2\alpha \approx 0°$).

6. SED APPROACH IN FRACTURE ANALYSIS OF THE TESTED PMMA SPECIMENS

The fracture criterion described in the previous section is employed here to estimate the fracture loads obtained from the experiments conducted on the PMMA specimens.

As originally thought for pure modes of loading the averaged strain energy density criterion states that failure occurs when the mean value of the strain energy density over a control volume $\bar{W}$ reaches a critical value W_c, which depends on the material but not on the notch geometry.

Under tension loads, this critical value can be determined from the ultimate tensile strength σ_t according to Beltrami's expression for the unnotched material:

$$W_{1c} = \frac{\sigma_t^2}{2E}. \qquad (14)$$

By using the values of σ_t = 70 MPa and E = 2950 MPa, the critical SED for the tested PMMA is W_{1c} = 0.83 MJ/m^3.

Under torsion loads, this critical value can be determined from the ultimate shear strength τ_t according to Beltrami's expression for the unnotched material:

$$W_{3c} = \frac{\tau_t^2}{2G}. \qquad (15)$$

By using the values of τ_t = 43 MPa and G = 1100 MPa, the critical SED for the tested graphite is W_{3c} = 0.84 MJ/m^3.

In parallel, the control volume definition via the control radius R_c needs the knowledge of the mode I and mode III critical notch stress intensity factor K_{Ic}^V and K_{IIIc}^V and the Poisson ratio ν, see Eqs. (12) and (13). For the considered material K_{Ic}^V and K_{IIIc}^V have been obtained from specimens weakened by sharp V-notches with an opening angle $2\alpha < 5°$ and a notch radius less than 0.1 mm. A precrack was also generated with a razor blade at the notch tip. The resulting values are K_{Ic}^V = 1.92 MPa × m$^{0.5}$ and K_{IIIc}^V = 1.40 MPa × m$^{0.5}$ which provide the control radii R_{1c} = 0.183 mm and R_{3c} = 0.324 mm, under pure tension and pure torsion, respectively.

The approach proposed here is a reminiscent of the work by Gough and Pollard [32] who proposed a stress-based expression able to summarize together the results obtained from bending and torsion. The criterion was extended in terms of the local SED to V-notches under fatigue loading in the presence of combined tension and torsion [33] and recently under static loading [37].

In agreement with [33, 37] and extending the method to the static case, the following elliptic expression:

$$\frac{W_1}{W_{1c}} + \frac{W_3}{W_{3c}} = 1 \qquad (16)$$

is obtained. In Eqs. (14) and (15) W_{1c} and W_{3c} are the critical values of SED under pure tension and pure torsion. For the considered graphite, W_{1c} = 0.83 MJ/m^3 and W_{3c} = 0. 84 MJ/m^3. Each specimen reaches its critical energy when the sum of the weighted contributions of mode I and mode III is equal to 1, which represents the complete damage of the specimen.

The values of W_1 and W_3 have, instead, to be calculated as a function of the geometry and of the applied mode mixity ratio, where K_I and K_{III} represent the mode I and mode III SIF ranges, R_{1c} and R_{3c} are the radii of the control volume related to mode I and mode III loadings, while e_1 and e_3 are equal to 0.11861 and 0.4138, respectively.

The detailed calculations employing this second criterion are reported in Table 2. The square root of the left-hand side term of Eq. (16), which is, in fact, proportional to the critical load, is given in the last column of this table.

Table 2. Experimental results. Overview of the data by using the proposed SED method

M	W_1, MJ/m^3	W_3, MJ/m^3	$W_1/W_{1c}+W_3/W_{3c}$	$(W_1/W_{1c}+W_3/W_{3c})^{1/2}$
0.00	0.83	0.00	1.00	1.00
0.00	0.89	0.00	1.07	1.03
0.00	0.94	0.00	1.14	1.07
0.00	0.91	0.00	1.09	1.05
0.19	0.66	0.12	0.94	0.97
0.19	0.73	0.13	1.04	1.02
0.19	0.81	0.15	1.15	1.07
0.19	0.71	0.13	1.01	1.00
0.48	0.33	0.57	1.07	1.04
0.48	0.35	0.62	1.15	1.07
0.48	0.38	0.66	1.23	1.11
0.48	0.36	0.63	1.18	1.09
0.51	0.37	0.75	1.33	1.16
0.51	0.39	0.80	1.41	1.19
0.51	0.41	0.84	1.49	1.22
0.51	0.38	0.77	1.37	1.17
0.78	0.06	0.93	1.17	1.08
0.78	0.06	0.93	1.17	1.08
0.78	0.06	0.96	1.20	1.10
0.78	0.06	0.95	1.19	1.09
1.00	0.00	0.92	1.08	1.04
1.00	0.00	0.94	1.10	1.05
1.00	0.00	0.97	1.14	1.07
1.00	0.00	0.95	1.12	1.06

A synthesis in terms of the square root value of the considered parameter, that is the sum of the weighted energy contributions related to mode I and mode III loading, is shown in Fig. 7 as a function of the mode mixity parameter $M = 2/\pi \arctan(K_{III}/K_I)$. Many of the results are inside a scatter band ranging from 0.9 to 1.1 with only few exceptions.

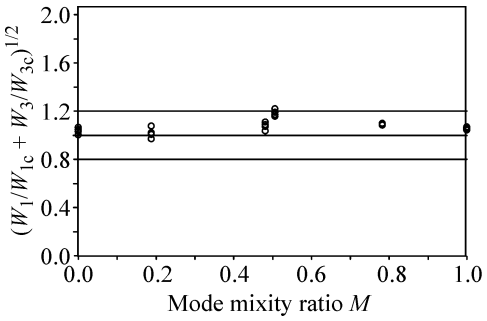

Fig. 7. Synthesis based on SED of the PMMA results from combined tension and torsion tests.

The fracture models proposed in this paper can be used for predicting the onset of brittle fracture in notched PMMA components which are subjected to a combination of tension and torsion loading.

7. CONCLUSIONS

Pure mode I, pure mode III and different intermediate mode I/III mixities fracture toughness values of commercial PMMA material were obtained experimentally using sharp notched ENDB specimens.

The proposed ENDB specimen in this research was capable of introducing the complete mixed mode I/III cases simply by changing the crack inclination angle relative to three-point bend rollers.

Although the fracture load of ENDB specimens made of PMMA was increased by moving from mode I

to mode III loading condition, the average mode I fracture toughness of tested specimen was about 30% greater than K_{IIIc} value.

Mixed mode I/III PMMA notch fracture toughness data were predicted successfully using the SED fracture criterion.

The SED approach has been found very suitable to summarize all the data in a narrow scatterband.

ACKNOWLEDGMENTS

The authors would like to thanks Mr. Farhad Zivari (Machining workshop, School of Industrial Engineering at Iran University of Science and Technology) for his helps in manufacturing the test specimens.

REFERENCES

1. Erdogan, F. and Sih, G.C., On the Crack Extension in Plates under Plane Loading and Transverse Shear, *J. Basic. Eng.*, 1963, vol. 85, no. 4, pp. 519–525.
2. Maccagno, T.M. and Knott, J.F., The Fracture Behaviour of PMMA in Mixed Modes I and II, *Eng. Fract. Mech.*, 1989, vol. 34, no. 1, pp. 65–86.
3. Aliha, M.R.M. and Ayatollahi, M.R., Geometry Effects on Fracture Behaviour of Polymethyl Methacrylate, *Mater. Sci. Eng. A*, 2010, vol. 527, no. 3, pp. 526–530.
4. Awaji, H., Kato, T., Honda, S., and Nishikawa, T., Criterion for Combined Mode I–II Brittle Fracture, *J. Ceramic Soc. Japan*, 1999, vol. 107, no. 10, pp. 918–924.
5. Ayatollahi, M.R., Aliha, M.R.M., and Hassani, M.M., Mixed Mode Brittle Fracture in PMMA—an Experimental Study Using SCB Specimens, *Mater. Sci. Eng. A*, 2006, vol. 417, no. 1, pp. 348–356.
6. Ayatollahi, M.R., Aliha, M.R.M., and Saghafi, H., An Improved Semi-Circular Bend Specimen for Investigating Mixed Mode Brittle Fracture, *Eng. Fract. Mech.*, 2011, vol. 78, no. 1, pp. 110–123.
7. Saghafi, H., Zucchelli, A., and Minak, G., Evaluating Fracture Behavior of Brittle Polymeric Materials Using an IASCB Specimen, *Polym. Test*, 2013, vol. 32, no. 1, pp. 133–140.
8. Aliha, M.R.M., Bahmani, A., and Akhondi, S., Mixed Mode Fracture Toughness Testing of PMMA with Different Three-Point Bend Type Specimens, *Eur. J. Mech. A/Solid*, 2016, vol. 58, pp. 148–162.
9. Ayatollahi, M.R. and Aliha, M.R.M., Analysis of a New Specimen for Mixed Mode Fracture Tests on Brittle Materials, *Eng. Fract. Mech.*, 2009, vol. 76, no. 11, pp. 1563–1573.
10. Richard, H.A., Some Theoretical and Experimental Aspects of Mixed Mode Fractures, *6 Int. Conf. on Fracture*, New Delhi, India, 1984.
11. Gómez, F.J. and Elices, M., Fracture of Components with V-Shaped Notches, *Eng. Fract. Mech.*, 2003, vol. 70, no.14, pp. 1913–1927.
12. Gómez, F.J. and Elices, M., A Fracture Criterion for Sharp V-Notched Samples, *Int. J. Fract.*, 2003, vol. 123, no. 3–4, pp. 163–175.
13. Gómez, F.J., Elices, M., and Planas, J., The Cohesive Crack Concept: Application to PMMA at –60°C, *Eng. Fract. Mech.*, 2005, vol. 72, no. 8, pp. 1268–1285.
14. Gómez, F.J., Elices, M., Berto, F., and Lazzarin, P., Local Strain Energy to Assess the Static Failure of U-Notches in Plates under Mixed Mode Loading, *Int. J. Fract.*, 2007, vol. 145, no. 1, pp. 29–45.
15. Susmel, L., and Taylor, D., The Theory of Critical Distances to Predict Static Strength of Notched Brittle Components Subjected to Mixed-Mode Loading, *Eng. Fract. Mech.*, 2008, vol. 75, no. 3, pp. 534–550.
16. Berto, F., Cendon, D.A., Lazzarin, P., and Elices, M., Fracture Behaviour of Notched Round Bars Made of PMMA Subjected to Torsion at –60°C, *Eng. Fract. Mech.*, 2013, vol. 102, pp. 271–287.
17. Ahmadi-Moghadam, B. and Taheri, F., An Effective Means for Evaluating Mixed-Mode I/III Stress Intensity Factors Using Single-Edge Notch Beam Specimen, *J. Strain Anal. Eng. Des.*, 2013, vol. 48, no. 4, pp. 245–257.
18. Liu, S., Chao, Y.J., and Zhu, X., Tensile-Shear Transition in Mixed Mode I/III Fracture, *Int. J. Solids Struct.*, 2004, vol. 41, no. 22, pp. 6147–6172.
19. Ayatollahi, M.R. and Saboori, B., A New Fixture for Fracture Tests under Mixed Mode I/III Loading, *Eur. J. Mech. A/Solids*, 2015, vol. 51, pp. 67–76.
20. Richard, H.A., Schramm, B., and Schirmeisen, N.H., Cracks on Mixed Mode Loading—Theories, Experiments, Simulations, *Int. J. Fatigue*, 2014, vol. 62, pp. 93–103.
21. Lazzarin, P. and Berto, F., Some Expressions for the Strain Energy in a Finite Volume Surrounding the Root of Blunt V-Notches, *Int. J. Fract.*, 2005, vol. 135, no. 1–4, pp. 161–185.
22. Lazzarin, P. and Zambardi, R., A Finite-Volume-Energy Based Approach to Predict the Static and Fatigue Behavior of Components with Sharp V-Shaped Notches, *Int. J. Fract.*, 2001, vol. 112, no. 3, pp. 275–298.
23. Aliha, M.R.M., Bahmani, A., and Akhondi, S., Numerical Analysis of a New Mixed Mode I/III Fracture Test Specimen, *Eng. Fract. Mech.*, 2015, vol. 134, pp. 95–110.
24. Aliha, M.R.M., Bahmani, A., and Akhondi, S., Determination of Mode III Fracture Toughness for Different Materials Using a New Designed Test Configuration, *Mater. Des.*, 2015, vol. 86, pp. 863–871.
25. Williams, M.L., Stress Singularities Resulting from Various Boundary Conditions, *J. Appl. Mech.*, 1952, vol. 19, no. 4, pp. 526–528.
26. Zappalorto, M., Lazzarin, P., and Berto, F., Elastic Notch Stress Intensity Factors for Sharply V-Notched Rounded

Bars under Torsion, *Eng. Fract. Mech.*, 2009, vol. 76, no. 3, pp. 439–453.
27. Zappalorto, M., Lazzarin, P., and Filippi, S., Stress Field Equations for U- and Blunt V-Shaped Notches in Axisymmetric Shafts under Torsion, *Int. J. Fract.*, 2010, vol. 164, no. 2, pp. 253–269.
28. Zappalorto, M., Lazzarin, P., and Yates, J.R., Elastic Stress Distributions for Hyperbolic and Parabolic Notches in Round Shafts under Torsion and Uniform Antiplane Shear Loadings, *Int. J. Solids Struct.*, 2008, vol. 45, no. 18, pp. 4879–4901.
29. Qian, J. and Hasebe, N., Property of Eigenvalues and Eigenfunctions for an Interface V-Notch in Antiplane Elasticity, *Eng. Fract. Mech.*, 1997, vol. 56, no. 6, pp. 729–734.
30. Berto, F., Lazzarin, P., Kotousov, A., and Harding, S., Out-of-Plane Singular Stress Fields in V-Notched Plates and Welded Lap Joints Induced by In-Plane Shear Load Conditions, *Fatigue Fract. Eng. Mater. Struct.*, 2011, vol. 34, no. 4, pp. 291–304.
31. Berto, F. and Lazzarin, P., Fatigue Strength of Structural Components under Multi-Axial Loading in Terms of Local Energy Density Averaged on a Control Volume, *Int. J. Fatigue*, 2011, vol. 33, no. 8, pp. 1055–1065.
32. Gough, H.J. and Pollard, H.V., Properties of Some Materials for Cast Crankshafts, with Special Reference to Combined Stresses, *Proc. Inst. Auto. Eng.*, 1963, vol. 31, no. 1, pp. 821–893.
33. Lazzarin, P., Sonsino, C.M., and Zambardi, R., A Notch Stress Intensity Approach to Assess the Multiaxial Fatigue Strength of Welded Tube-to-Flange Joints Subjected to Combined Loadings, *Fatigue Fract. Eng. Mater. Struct.*, 2004, vol. 27, no. 2, pp. 127–140.
34. Lazzarin, P., Berto, F., Elices, M., and Gómez, J., Brittle Failures from U- and V-Notches in Mode I and Mixed, I + II, Mode: A Synthesis Based on the Strain Energy Density Averaged on Finite-Size Volumes, *Fatigue Fract. Eng. Mater. Struct.*, 2009, vol. 32, no. 8, pp. 671–684.
35. Berto, F. and Lazzarin, P., A Review of the Volume-Based Strain Energy Density Approach Applied to V-Notches and Welded Structures, *Theor. Appl. Fract. Mech.*, 2009, vol. 52, no. 3, pp. 183–194.
36. Berto, F. and Lazzarin, P., Recent Developments in Brittle and Quasi-Brittle Failure Assessment of Engineering Materials by Means of Local Approaches, *Mater. Sci. Eng. R. Rep.*, 2014, vol. 75, pp. 1–48.
37. Berto, F., Campagnolo, A., and Ayatollahi, M.R., Brittle Fracture of Rounded V-Notches in Isostatic Graphite under Static Multiaxial Loading, *Phys. Mesomech.*, 2015, vol. 18, no. 4, pp. 283–297.